JOURNAL OF CATALYSIS **164,** 44–53 (1996)
ARTICLE NO. 0361

The Effect of Reaction Conditions and Time on Stream on the Coke Formed during Propane Dehydrogenation

Mikael Larsson,* Magnus Hultén,† Edd A Blekkan,‡ and Bengt Andersson*,[1]

*Department of Chemical Reaction Engineering, Chalmers University of Technology, S-412 96 Göteborg, Sweden; †Department of Heat and Power Technology, Chalmers University of Technology, S-412 96 Göteborg, Sweden; ‡Department of Industrial Chemistry, The Norwegian University of Science and Technology, N-7034 Trondheim, Norway

Received October 30, 1995; revised August 2, 1996; accepted August 5, 1996

Pt/Al_2O_3 and Pt–Sn/Al_2O_3 catalysts, coked during propane dehydrogenation, have been studied using temperature-programmed oxidation (TPO). Time on stream, temperature, and reaction gas composition have been varied. Three different peaks were identified from the TPO profiles on the Pt–Sn catalyst and attributed to different types of coke; coke on and in the vicinity of the metal, coke on the carrier, and graphitic coke on the carrier. The amounts of these types were related to reaction conditions. The formation of the coke belonging to the first two peaks in the TPO profiles increases with temperature and partial pressure of propene. Hydrogen, on the other hand, suppresses the formation. The amount of coke that can be attributed to the third peak increases with temperature and propane partial pressure. A model is discussed where a minor part of the coke deactivates the catalyst. This coke is formed in parallel with the coke that is seen in the first two peaks in the TPO experiments. The graphitic coke formed on the carrier is not formed through this route. The experiments with different time on stream revealed that the first peak reached a constant level after about 15 h, while the second one still increased. Hydrogen was very efficient in preventing coke formation and deactivation but could not remove coke already formed on the catalyst. The hydrogenolysis and cracking mechanisms during the propane dehydrogenation are also discussed.

INTRODUCTION

The addition of tin to a platinum catalyst has proved to be an effective way to reduce undesired reactions and prevent deactivation, due to coke formation in naphtha reforming and alkane dehydrogenation reactions (1–5). Therefore, the bimetallic platinum-tin catalyst has received considerable attention in the last few decades. The goal in most investigations carried out with Pt and Pt–Sn catalysts has been to study the performance in the reforming process. However, dehydrogenation of light paraffins is commercially done at a relatively high temperature, 770–900 K (6), and the deactivation rate and coke formation may differ from those in experiments conducted at lower temperatures.

Many authors have studied the effect of tin in the formation and composition of the coke by temperature-programmed oxidation (TPO) (5, 7–13). The different peaks found in the TPO profiles have been proposed to be coke with different locations and different composition. The effect of the catalyst composition, for example loading of tin, on the coke formed has been investigated in great detail (9). When tin is added to a Pt/Al_2O_3 catalyst, an increased total amount of coke is usually found (1, 4, 5, 14, 15). The hydrogen to carbon ratio of the coke and the relation of the different peaks in the TPO profiles have also been analyzed, but often with contradicting results (5, 7, 9, 12, 13, 16).

The issues we have tried to address in this study are: how will the deactivation change over time and with altered reaction conditions; are different types of coke formed; and if so, does the ratio between the types depend on the conditions; and how does the coke influence the catalyst. In this paper we present two different studies of deactivated Pt/Al_2O_3 and Pt–Sn/Al_2O_3 dehydrogenation catalysts, where the coke has been deposited using different reaction conditions. In the first study, the reaction conditions were held constant except for the deactivation time. In the second set of experiments, deactivation time has been kept constant but reaction conditions such as flows and temperatures have been changed.

METHODS

Pt/Al_2O_3 and Sn/Al_2O_3 catalysts were prepared by incipient wetness impregnation of a commercial γ-alumina support with aqueous solutions containing either H_2PtCl_6 or $SnCl_2$. The bimetallic Pt–Sn catalyst was prepared from the calcined Sn/Al_2O_3 catalyst by impregnation with H_2PtCl_6. Table 1 shows data from the characterization of the catalysts. The details of preparation and characterization can be found elsewhere (17).

---

[1] Author to whom correspondence should be addressed: Fax: +46 31 772 30 35; E-mail: bengt@cre.chalmers.se. http://www.che.chalmers.se/inst/cre/krthem.htm.

0021-9517/96 $18.00

TABLE 1

Catalyst Properties

Catalyst	Particle size	Pt loading[a]	Sn loading[a]	Dispersion[b]	BET surface
Pt/Al_2O_3	0.05–0.14 mm	0.85 wt%	—	13%	162 m^2/g
Pt–Sn/Al_2O_3	0.05–0.14 mm	0.74 wt%	1.53 wt%	29%	172 m^2/g

[a] By atomic absorption spectrometry.

[b] By hydrogen chemisorption in a volumetric system assuming H : Pt = 1 : 1.

TPO after Different Times on Stream

Deactivation during different times on stream (TOS) followed by temperature-programmed oxidation was carried out in the microbalance reactor consisting of a tubular quartz reactor (15 mm i.d.) fitted to the balance (CI Electronics Mark 2B).

The catalyst (approx. 55 mg) was placed in a quartz basket (6 mm i.d.) and suspended from the balance using thin quartz fibers. The reactor was heated in a vertical electrical furnace, controlled by a thermocouple located immediately below the basket. Mass flow controllers (Bronkhorst HI-TEC) regulated the gas flows. All experiments in the reactor were performed at atmospheric pressure. For further details of the reaction setup, see (18).

Reduction was carried out prior to the coking in N_2: 20 ml/min and H_2: 10 ml/min. A ramp from room temperature to the reduction temperature (789 K), at a speed of 4 K/min, was used. The catalyst was then kept at this temperature for 4 h.

After the reduction, propane and propene were added to the flow of nitrogen and hydrogen at 789 K. To avoid concentration gradients in the catalyst bed, an equilibrium mixture of propane, propene, and hydrogen, diluted with nitrogen, was used to generate the coke deposition on the catalysts (C_3H_8: 20.3 ml/min, C_3H_6: 7.5 ml/min, H_2: 7.5 ml/min, and N_2: 64.7 ml/min). The coking was carried out for different times on stream (from 5 min to 41.5 h).

After the deactivation the reactor was cooled to room temperature in N_2. The TPO experiment was then immediately performed in the same reactor without exposing the catalyst to the moisture in the air. The rate of the temperature ramp was 10 K/min and 5% O_2 was used (O_2: 5 ml/min, N_2: 95 ml/min). The TPO was allowed to continue until a final temperature of about 920 K was reached.

In some experiments, the effects of hydrogen on a coked catalyst were studied by flushing hydrogen through the reactor for 30 min immediately after the coking at the reaction temperature. The experiments were then continued by TPO.

TPO after Different Deactivation Conditions

The propane dehydrogenation and the TPO experiments were performed in a fully automated flow reactor system. The system was equipped with a GC-MS system (TRIO-1) and a GC with a flame ionization detector (Shimadzu, GC-mini 3 with a Chrompack, Plot fused silica Al_2O_3/KCl, column). The setup had two main gas lines, and an air-actuated four-way valve made it possible to switch quickly between these two flows. The hydrocarbons were analyzed during the propane dehydrogenation using the GC. The MS in the GC-MS system was used to follow the CO_2 signal at m/e 44 and to confirm the absence of uncombusted hydrocarbons and CO. Mass flow controllers (Bronkhorst HI-TEC) controlled the gas flow rates.

The 19 propane dehydrogenation experiments were performed as a full factorial design of experiments (19) with four independent variables, one center point, and two additional experiments at the center point conditions but at the lower temperature. The total flow rate was always 50 ml/min and the pressure atmospheric. The levels of the variables are shown in Table 2 and the whole design can be found in Table 3.

About 100 mg of the catalyst was reduced in flowing hydrogen for 145 min at 841 K. After this the temperature of the system was adjusted to the reaction temperature and allowed to stabilize for 20 min before the flow was switched to the reaction mixture. For all experiments the total time on stream was 10 h, and the reaction conditions were kept constant during each run.

After the propane dehydrogenation reaction, the reactor was cooled down and a TPO experiment was performed in the same apparatus. A gas mixture of 2% O_2 in Ar at a total flow rate of 25 ml/min was used. The heating rate was 10 K/min up to 1123 K. After the TPO experiment the heated catalyst was used to burn a mixture containing acetylene and oxygen in argon. Details about this calibration procedure that made it possible to determine the amount of coke on the catalyst can be found elsewhere (20).

Measurement of the Free Metal Surface Using CO Adsorption

The effect of hydrogen treatment on the coke covering the metal surface was also studied. This was done in the fixed-bed reactor. After reduction, the Pt catalyst was deactivated using the same flow rates as in the experiments conducted in the microbalance for 13 h. After the deactivation, temperature-programmed hydrogenation was performed;

TABLE 2

Levels of the Variables Used in the Factorial Experiment

Variable	Low level (−)	High level (+)	Center point (0)
Flow of H_2	2.4 ml/min	3.6 ml/min	3.0 ml/min
Flow of C_3H_8	7.6 ml/min	11.4 ml/min	9.5 ml/min
Flow of C_3H_6	1.6 ml/min	2.4 ml/min	2.0 ml/min
Temperature	789 K	841 K	815 K

TABLE 3

Design of and Results from the Factorial Experiment

Experiment number[a]	Flow rates (ml/min)				Temperature (K)	Turnover frequency (moles/(moles surface Pt ∗ s))						C_{1+2} (wt%)	C_3 (wt%)
						Initial TOF[b]					TOF after 10 h		
	H_2	C_3H_8	C_3H_6	N_2		C_3H_8 conversion	C_3H_6 formation	CH_4 formation	C_2H_4 formation	C_2H_6 formation	C_3H_8 conversion		
1	2.4	7.6	1.6	38.4	789	0.7724	0.7473	0.0099	0.0021	0.0096	0.1923	1.38	0.18
2	3.6	7.6	1.6	37.2	789	0.5576	0.5459	0.0126	0.0018	0.0123	0.2832	0.97	0.08
3	2.4	11.4	1.6	34.6	789	1.1946	1.1466	0.0118	0.0023	0.0110	0.3124	1.35	0.12
4	3.6	11.4	1.6	33.4	789	0.9440	0.8659	0.0121	0.0017	0.0114	0.4949	0.93	0.15
5	2.4	7.6	2.4	37.6	789	0.5721	0.5351	0.0107	0.0027	0.0100	0.0900	1.88	0.17
6	3.6	7.6	2.4	36.4	789	0.3515	0.3283	0.0109	0.0018	0.0104	0.1144	1.12	0.13
7	2.4	11.4	2.4	33.8	789	1.0267	0.9522	0.0130	0.0028	0.0121	0.1706	2.19	0.20
8	3.6	11.4	2.4	32.6	789	0.7563	0.7008	0.0117	0.0021	0.0107	0.2578	1.32	0.16
9	2.4	7.6	1.6	38.4	841	1.4587	1.3916	0.0313	0.0123	0.0238	0.1832	5.56	0.80
10	3.6	7.6	1.6	37.2	841	1.4076	1.3446	0.0334	0.0097	0.0277	0.3869	3.47	1.08
11	2.4	11.4	1.6	34.6	841	2.3834	2.3191	0.0441	0.0119	0.0368	0.3747	5.11	1.23
12	3.6	11.4	1.6	33.4	841	2.0339	1.9443	0.0460	0.0110	0.0386	0.6538	5.43	1.28
13	2.4	7.6	2.4	37.6	841	1.2407	1.1543	0.0298	0.0133	0.0219	0.0669	7.94[c]	
14	3.6	7.6	2.4	36.4	841	1.1039	0.9964	0.0318	0.0120	0.0249	0.1560	5.25	0.87
15	2.4	11.4	2.4	33.8	841	2.0208	1.9452	0.0377	0.0131	0.0290	0.1423	8.36[c]	
16[d]	3.6	11.4	2.4	32.6	841	0.9882	0.9209	0.026	0.0162	0.0119	0.0561	—	—
17	3	9.5	2	35.5	789	0.7321	0.6933	0.0116	0.0022	0.0107	0.1822	1.16	0.33
18	3	9.5	2	35.5	789	0.7775	0.7399	0.0126	0.0022	0.0118	0.2265	1.47	0.29
19	3	9.5	2	35.5	815	1.3272	1.1824	0.0217	0.0056	0.0208	0.1397	2.45	0.53

[a] The experiments were carried out in randomized order.
[b] The initial TOFs were calculated by extrapolation to time = 0.
[c] One broad peek was detected in the TPO experiment. The total coke content is given.
[d] The experiment was unsuccessful and the data was not used in the analysis.

i.e., the catalyst was treated in a hydrogen-containing gas mixture (H_2: 5.0 ml/min and N_2: 10 ml/min) during a temperature ramp (20 K/min) to 773 K. The reactor was kept at 773 K for 30 min and then cooled again. The free metal surface was studied by carbon monoxide absorption (21) on fresh, deactivated, and hydrogenated catalyst.

RESULTS AND DISCUSSION

TPO after Different TOS

Figure 1 shows the weight increase for different runs with the Pt/Al_2O_3 and $Pt\text{–}Sn/Al_2O_3$ catalysts as solid lines. More coke accumulates on the latter catalyst, which is consistent with earlier findings (1, 4, 5, 14, 15). The coke accumulation is very fast in the beginning, but slows down and reaches a more constant rate after about 5 h.

The TPO experimental results are shown in Fig. 2. Two peaks were observed after the monometallic Pt/Al_2O_3 catalyst had deactivated for at least 5 h. For the bimetallic $Pt\text{–}Sn/Al_2O_3$ catalyst, a shoulder was seen on the larger peak. For both catalysts the peak temperatures shifted upwards when the deactivation increased. Also, more severe coking caused the beginning of the gasification to shift to higher temperature.

Duprez *et al.* (22) studied how the different peaks in TPO profiles, derived from a Pt/Al_2O_3 catalyst coked by cyclopentane at 673 K, changed with time on stream. They identified three different peeks, and showed that the first peak (543–593 K) disappears when the temperature during coking is increased to at least 753 K (23). They conclude

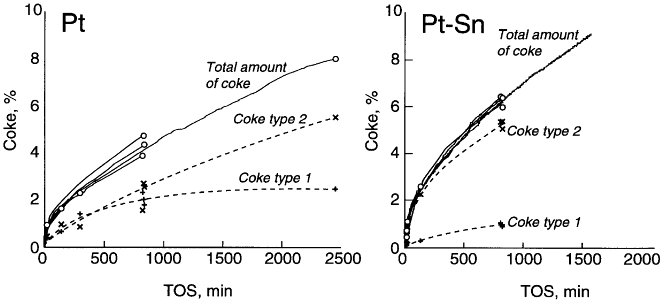

FIG. 1. Long-time coke formation on the platinum and the platinum–tin catalysts. The amounts of the different types of coke are calculated from the TPOs: (◯) total amount of coke; (+) coke type 1; (x) coke type 2. The solid lines show the weight monitored by the microbalance and the dashed lines are estimations from the TPO data. The gas mixture contained 20.3 ml/min C_3H_8, 7.5 ml/min C_3H_6, 7.5 ml/min H_2, and 40 ml/min N_2. The temperature was 789 K.

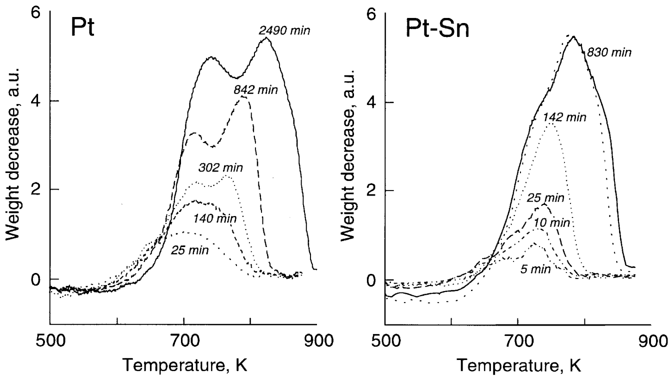

FIG. 2. Temperature-programmed oxidation performed in the microbalance after different times on stream on the platinum and the platinum–tin catalysts (Fig. 1).

that the peak shifts to a higher temperature due to a larger degree of graphitization of the coke on the metal, at the elevated temperature. The shape of the peaks on the catalyst deactivated at 773 K by Duprez *et al.* (23) is similar to the ones in Fig. 2 for the monometallic Pt/Al_2O_3 catalyst.

We agree with a model, earlier proposed by others (10, 22, 24, 25), that only a small part of the coke is located on the metal, while a larger part is placed close to the metal and is assisted by the platinum in the combustion. We believe that the last part of the coke is deposited on the carrier and is combusted without any influence by the metal.

Lin *et al.* (8) identified two different types of coke when comparing Pt/Al_2O_3 and $Pt–Sn/Al_2O_3$. Our results are consistent with their findings that the relation between the two peaks is different for the Pt and the Pt–Sn catalysts. Relatively more coke belongs to the first peak on the former catalyst than it does on the latter one. The same effect has also been observed for platinum catalysts modified with Re and Ir (26).

Lok *et al.* (16) have discussed the role of coke accumulated in the metal-carrier boundary. They found that the coking rate consists of two regimes, just as that in this study. The coke formation rate is very high in the beginning of the run, but later reaches a regime with a lower, almost constant rate. Lok *et al.* (16) proposed a model where coke precursors migrate to the boundary between the platinum and the carrier. They suggested that when most of the sites in the boundary are being occupied, the coke formation rate is reduced. It was also proposed that the role of tin is to improve the migration of coke and coke precursors from the metal and the metal-carrier boundary to the carrier.

The bimetallic Pt–Sn catalyst is more resistant to deactivation by coke formation, than the monometallic Pt. Lieske *et al.* (27) and Lin *et al.* (8) suggest that one reason is that hydrocarbons bind more strongly to Pt/Al_2O_3 than to $Pt–Sn/Al_2O_3$. If the first peak in the TPO spectra was caused by coke being deposited on the metal and in the metal-support boundary, then the weakened metal-hydrocarbon binding by the addition of tin, would explain the significant reduction of the first peak.

The TPO experiments performed in the microbalance were deconvoluted using a model with a combination of power-law kinetic expressions, proposed and discussed in detail by Querini and Fung (28). Two different types of cokes (type 1 and 2, from the low and the high temperature peaks, respectively) and constant oxygen pressure were assumed. The reason for the latter assumption is the excess of oxygen used in the experiment. The results from the deconvolution are incorporated in Fig. 1.

Figure 1 demonstrates how the coke, associated with peak 1, increases in the beginning, but reaches a constant level after a period of deactivation. In contrast, the second type of coke increases continuously.

We suggest that a part of the coke belonging to peak 1 is responsible for the deactivation of the active sites on the metal and that it hinders the transport of coke precursors to the support which thus increases the coke accumulation on the platinum. The addition of tin to the platinum catalyst reduces the metal–carbon bond, leaving a larger metal surface free (8, 17), and promotes the migration of coke precursors to the carrier.

The change in gas composition from the reaction mixture to hydrogen at the reaction temperature did not affect the weight of the coke. The TPO curves from the runs, where the catalysts were exposed to hydrogen after the reaction, were compared with experiments without hydrogen treatment for approximately the same TOS. No systematic differences were found.

The experiments, where the free metal surface was measured on fresh and deactivated catalyst and on catalyst exposed to hydrogen, showed that the free metal surface on the deactivated Pt/Al_2O_3 catalyst was not changed significantly by treatment with hydrogen at 773 K. Fresh catalyst adsorbed 2.4 μmol CO/g catalyst, and both the deactivated catalyst and the deactivated catalyst treated with hydrogen absorbed about 0.05 μmol CO/g catalyst. The conclusion from the different experiments with hydrogen treatment of coked catalysts must be that hydrogen has little effect on the coke formed during the experiments.

TPO Profiles after Different Reaction Conditions

All experiments were done using the same amount of the $Pt–Sn/Al_2O_3$ catalyst, the same total flow rate and a total time on stream of 10 h. Figure 3 shows an example of a run and additional data can be found in Table 3.

The amount of coke on the catalyst varied from about 1 to 8 wt%. Examples of typical TPO profiles can be found in Fig. 4a, and two or three different peaks can be identified in the curves. The high temperature peak of about 950 K is seldom found on catalysts. However, by reacting 1,5-hexadiene on γ-alumina at 723 K, Sárkány *et al.* (10) achieved one single peak with a maximum at about

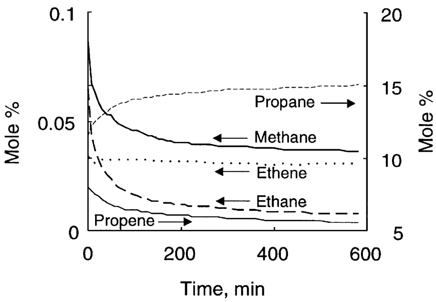

FIG. 3. The gas concentrations in a typical experiment (experiment 13 in Table 3).

980 K. They did not find this peak for catalysts containing platinum. By IR studies on the coked alumina carrier they found condensed aromatic ring compounds. Bacaud *et al.* (29) detected a peak with a maximum at around 1000 K for graphite mixed mechanically with a Pt/Al_2O_3 catalyst. The peak at 950 K in Fig. 4a is probably from the coke with a graphitic structure, which is mainly formed under severe conditions.

The TPO profiles were deconvoluted using Gaussian curves assuming two or three different types of coke. An example of the latter case is found in Fig. 4b. The fit was excellent for all the experiments apart from the two with higher coke loadings (8 wt%). In those experiments one very broad peak was observed because of the lack of oxygen, and/or mass transfer limitations. These two experiments were omitted in the analysis of the different peaks. In the following analysis the first two types of coke were treated together, named C_{1+2}, and the last type separately, C_3. The major part of the coke belonged to the first two types of coke.

The data from the TPO experiments and the GC analysis were used in a linear regression analysis. Linear models of the type shown in Eq. [1] have been tested:

$$y = b_0 + b_1x_1 + b_2x_2 + b_{12}x_1x_2. \qquad [1]$$

In the analysis, the independent variables were centered and scaled to the range −1 to 1, and the significance was tested for all linear predictor variables and cross-products.

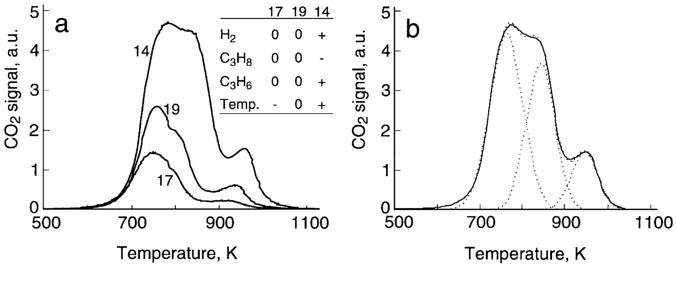

FIG. 4. (a) Example of TPO profiles for catalysts deactivated at reaction conditions found in Table 2. The numbers in the figure refer to Table 3. (b) Example of deconvolution using Gaussian curves for experiment 14.

Furthermore, the experimental design, an almost orthogonal plan, made model-building very simple. The data concerning the amount of coke, were analyzed separately at high and low temperature, because the absolute errors were much larger for the high temperature. The temperature is by far the most important variable controlling the formation of coke. In fact, more than four times as much coke was formed at the high temperature.

Separate analyses were performed for the different types of coke. The first two peaks were treated as a sum, C_{1+2}. The model for C_{1+2} as a function of the gas flow rates can be found in Fig. 5a for the experiments performed at low temperature. A corresponding model with significant parameters was not possible to achieve for the experiments performed at the high temperature, although the relationship was similar. In Fig. 5 (and also Figs. 6 and 11) nonsignificant variables have been left out. Only the flows of hydrogen (decrease in C_{1+2}) and propene (increase in C_{1+2}) influenced the formation of coke C_{1+2}. The amount of the third type of coke was also studied as a function of the flow rates. For the low temperature no correlation was found. For the high temperature it was possible to relate the propane flow to C_3, as shown in Fig. 5b. Because the partial pressure of propane is several times larger than the partial pressure of propene in the experiments, it was difficult to determine if it was the sum of the hydrocarbons or only propane that caused the formation of C_3.

The coke selectivity, defined as carbon on the catalyst per carbon converted, was also analyzed in the same way. The model can be found in Fig. 6a. It is obvious that adding propene increases the coke selectivity by reducing the dehydrogenation rate and increasing the coke formation. Again, it is obvious why adding propane will decrease the coke selectivity. However, it is worth noting that adding hydrogen decreases the coke selectivity, because the coke prevention effect is larger than the inhibition of the reaction rate. Increasing the temperature will cause much more coke and, even if the propane conversion increases, the first effect is more pronounced, and the coke selectivity increases.

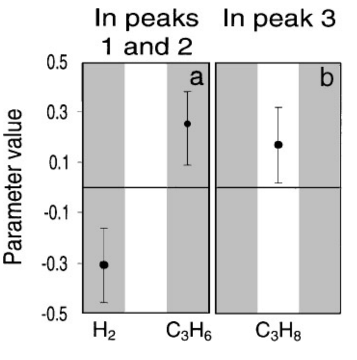

FIG. 5. The amount of coke in (a) C_{1+2} at low temperature and (b) C_3 at high temperature vs gas composition. The parameter values, with 95% confidence intervals, obtained in the linear regression analyses.

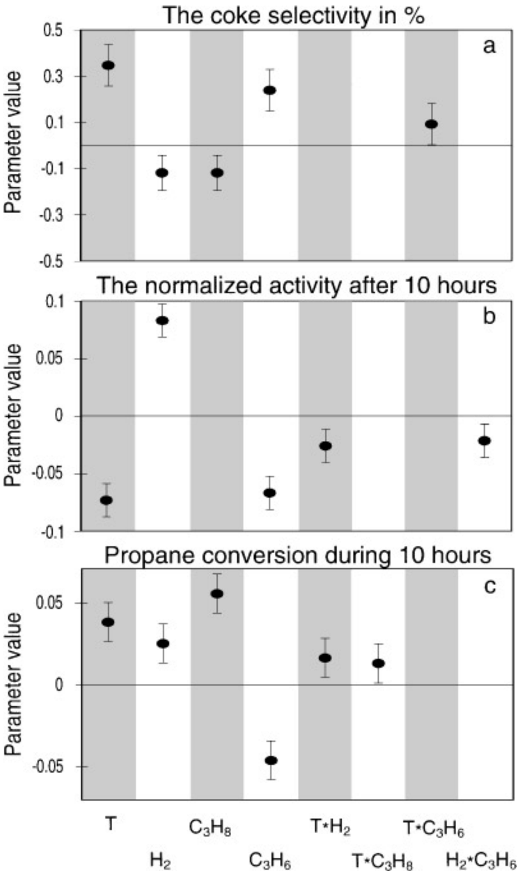

FIG. 6. The parameter values, with 95% confidence intervals, obtained in the linear regression analyses of: (a) the coke selectivity; (b) the normalized activity, γ_{10}; (c) the propane conversion during 10 h; all vs reaction conditions.

We have correlated the deactivation rate with the experimental conditions and the amount of coke. First, a model for the normalized activity (γ_{10}); i.e., the ratio between the activity for propane dehydrogenation after 10 h on stream and the initial activity, related to the experimental conditions, was obtained (see Fig. 6b). It was found that hydrogen helps maintain the activity. However, increased propene partial pressure and higher temperature increased the deactivation. Next, a model relating the propane conversion integrated over 10 h to the experimental conditions was derived (see Fig. 6c). It showed that even if the addition of hydrogen was expected to decrease the initial conversion, the conversion integrated over the whole time period increased when the high hydrogen level was used. This effect was more pronounced at the high temperature.

It was also possible to relate the deactivation to the amount of coke. In Fig. 7a the normalized activity after 10 h (γ_{10}) has been plotted against the sum of coke one and two (C_{1+2}) after 10 h. The equations for the lines are

$$\gamma_{10} = e^{-bm_{\text{coke}}}, \qquad [2]$$

where b is a constant determined by regression, and m_{coke} is the amount of coke in weight percent. The equations have been determined separately for the high and the low temperatures. The same graphs are made for coke of type three (see Fig. 7b). The lower curves in the figures belong to ethane activity.

There are at least three explanations for why the relation between deactivation and amount of coke one and two follows one line for each temperature (see Fig. 7a). First, it is possible that the catalyst withstands more coke at the same degree of deactivation at the higher temperature because the nature of the coke is different. The second explanation is that the nature of the coke is unchanged, but that the effect of the coke is different when the reaction is carried out at the higher temperature. Finally, it is possible that only a small part of the coke causes the deactivation, and that the major part of the coke has hardly any effect on the activity. The formation of this main part of the coke, the part determined in TPO, is a function of activity and the present reaction conditions, and the formation is not directly coupled to the deactivation mechanism.

In order to examine which explanation is correct, propane dehydrogenation was carried out at different temperatures. After a time of deactivation, the temperatures were changed to a reference temperature (789 K), keeping the gas phase composition constant. The reaction conditions and initial activities are given in Table 4. In Fig. 8, the activity of propene formation has been normalized by dividing with initial activity. The vertical lines indicate that the temperatures were changed to the reference temperature, and the activity been related to the initial activity for the experiment performed at 789 K.

Figure 8 indicates that the degree of deactivation remained almost unchanged when the temperature was changed. The explanation proposed above, that the nature of the coke would change with reaction temperature, cannot be correct. If so, then the normalized activity would have changed considerably. Also the second explanation, that the nature of the coke is the same, but the effect of the coke changes with reaction temperature, would demand a considerable change in degree of deactivation with changing the temperature.

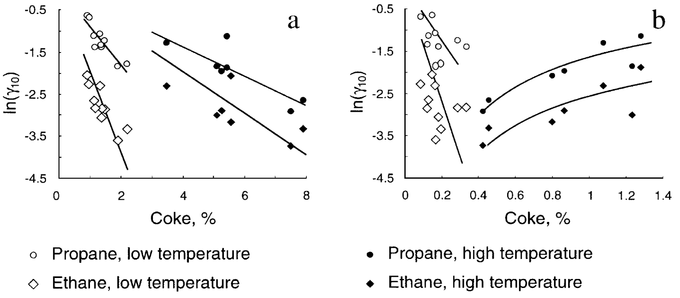

FIG. 7. The normalized activity after 10 h on stream, γ_{10}, for propane conversion and ethane formation vs (a) the sum of coke one and two, (b) coke of type three. Reaction conditions in Table 3.

TABLE 4

Reaction Conditions and Initial Turnover Frequencies in the Experiments, Where the Effect of the Temperature on the Deactivation Was Studied (Fig. 8)

Experiment number	Flow of H_2 (ml/min)	Flow of C_3H_8 (ml/min)	Flow of C_3H_6 (ml/min)	Flow of N_2 (ml/min)	Temperature (K)	Initial TOF, C_3H_8 conversion[a] (moles/(moles surface Pt $*$ s))
20	3	9.5	2	35.5	781	0.8062
21	3	9.5	2	35.5	789	1.023
22	3	9.5	2	35.5	815	1.449
23	3	9.5	2	35.5	849	2.459

[a] The initial TOFs were calculated by extrapolation to time = 0.

We suggest that the major part of the coke is not responsible for the deactivation. Instead we propose a model where the coke active in deactivating the catalyst is formed in parallel with the main coke formation. Figure 9 illustrates a possible reaction scheme in this case. The coke precursor is considered to be formed from the products, but the following discussion would also be valid if the coke was formed from a reactant or an intermediate. The coke precursor may be formed either in a reversible or irreversible reaction. Coke A is the main part of the coke formed during the reaction, but it is not responsible for the deactivation. Coke B is the coke that causes the deactivation of the catalyst. This part of the coke is small and cannot be distinguished in the TPO experiments.

If we assume that the deactivation is caused by Coke B in Fig. 9, the change in normalized activity γ over time can be written as

$$\frac{d\gamma}{dt} = -k_{\mathrm{CB}}\gamma\ f(CP), \qquad [3]$$

where k_{CB} is a constant and $f(CP)$ is any function of the precursor concentration on the catalyst. The differential equation can be solved for the reaction time 10 h and since $\gamma = 1$ at time = 0, the following expression is derived:

$$\ln(\gamma_{10}) = -k_{\mathrm{CB}} \int_0^{10\,\mathrm{h}} f(CP)dt. \qquad [4]$$

The reaction rates for the formation of the nondeactivating Coke A, can be expressed as

$$r_{\mathrm{CA}} = k_{\mathrm{CA}}\, f(CP). \qquad [5]$$

Earlier has the activity been related to the amount of coke by

$$\ln(\gamma_{10}) = -bm_{\mathrm{coke}}, \qquad [6]$$

where b was the slope in Fig. 7a. If we consider the amount of coke to be formed according to Eq. [5] and also uses the expression for $\ln(\gamma_{10})$ in Eq. [4], we achieve the following expression for b:

$$b = \frac{-\ln(\gamma_{10})}{m_{\mathrm{coke}}} = \frac{k_{\mathrm{CB}} \int_0^{10\,\mathrm{h}} f(CP)dt}{k_{\mathrm{CA}} \int_0^{10\,\mathrm{h}} f(CP)dt} = \frac{k_{\mathrm{CB}}}{k_{\mathrm{CA}}}. \qquad [7]$$

We can now explain the straight lines in Fig. 7 for the first types of coke by the constant ratio in the equation above because the change in gas composition will not change the ratio. It is important to stress that the deactivation times were the same in all experiments and that different deactivation times would not result in a straight line in Fig. 7a. A difference in activation energies, where $E_{\mathrm{CA}} > E_{\mathrm{CB}}$, would account for the different slopes at different temperatures. We know that the rate of the coke precursor formation, r_{CP} in Fig. 9, is related to the gas composition. The use of a high hydrogen and low propene partial pressure will decrease the formation, resulting in less coke and less deactivation. This can also be seen from the models presented in Figs. 5a and 6b.

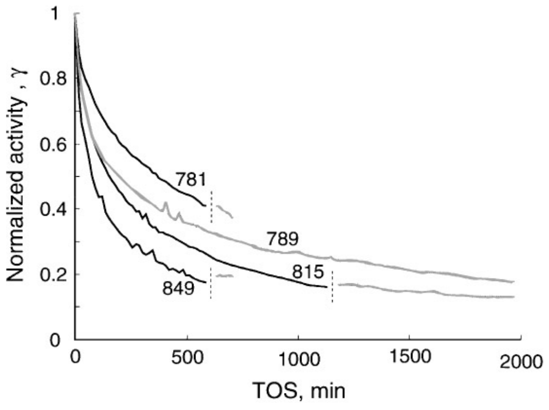

FIG. 8. The normalized propane dehydrogenation activity at different temperatures. The vertical lines indicate that the temperatures were changed to 789 K during the run, and that the activities are related to the initial activity for the run carried out at 789 K. Reaction conditions in Table 4.

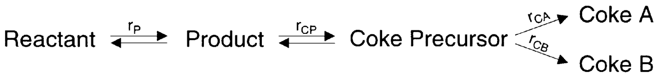

FIG. 9. A possible mechanism for deactivation and coke formation.

For the coke in peak three, the results differ. For the low-temperature experiments, the activity versus coke function follows the equation above, although more scattered (Fig. 7b). However, for the experiments performed at the high temperature, the activity is higher for higher amount of coke and follows the equation,

$$\gamma_{10} = bm_{\text{coke}} + c, \qquad [8]$$

where b and c are constants.

The third type of coke found, C_3, is not formed by the mechanism stated in Fig. 9. It is probably formed by a direct route from propane (and perhaps also from propene). This explains both why a more active catalyst can contain more coke and why only the temperature and the propane flow were important in the formation of the coke (Fig. 5b).

Deactivation of Ethane and Ethene Formation

We also studied the deactivation of the side reactions for ethene and ethane formation. Both ethene and ethane must be formed by some kind of cracking of C_3 because the sum of ethane and ethene production is equal to the formation of methane, except for the first 15 min. As seen in Fig. 3, the ethene formation is almost constant over the whole time period. But on the other hand, the ethane production deactivates very fast. The ethane production graph (see Fig. 10) shows three groups: (1) high temperature and high level of propane; (2) high temperature and low level of propane; and finally (3) low temperature. The activity remains almost constant and even increases for some experiments done at the higher temperature. In Fig. 11 the deactivation of ethane production has been related to the experimental conditions. The model showed that for the deactivation of ethane formation, in contrast to the deactivation of propene production, the temperature is not a significant parameter. The deactivation rate of ethane formation is also faster than the deactivation rate for propane dehydrogenation.

A correlation of ethene formation activity with amount of coke cannot be obtained. The ethane formation activity, on the other hand, can be related to the amount of coke. In the latter case, the situation is very much the same as for propane dehydrogenation, Figs. 7a and 7b, except that the deactivation is even more pronounced. If Eq. [7] is applied to the ethane formation, the steeper slopes, resulting in higher values on the constant b, are explained by a higher k_{CB} in the ethane formation than in the propane dehydrogenation. The absence of temperature dependence in the deactivation rate indicates that the activation energy, E_{CB}, for the deactivation during the ethane formation is close to zero.

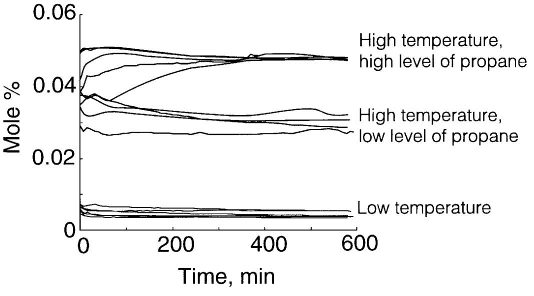

FIG. 10. The ethene production in all runs. The experiment that is slowly increasing is the one with high levels in all variables (experiment 16 in Table 3).

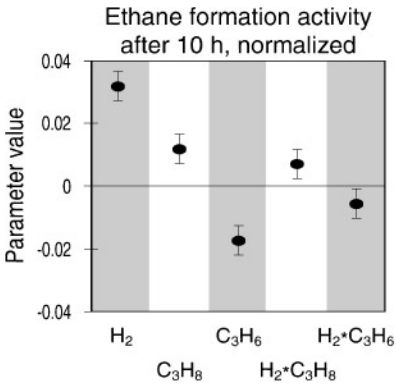

FIG. 11. The parameter values, with 95% confidence intervals, obtained in the linear regression analyses of the normalized ethane formation activity vs reaction conditions.

We have earlier investigated the formation of ethane and ethene during propane dehydrogenation under different reaction conditions (17). Pt/Al_2O_3, $Pt{-}Sn/Al_2O_3$, Sn/Al_2O_3, and Al_2O_3 catalysts were studied (see Fig. 12). The results showed a very slow deactivation of the ethene formation reaction on the Pt–Sn catalyst. The activity was higher for both the ethene and ethane formation on the monometallic catalyst than on the bimetallic one. The presence of tin decreased both the ethane and ethene formation also when

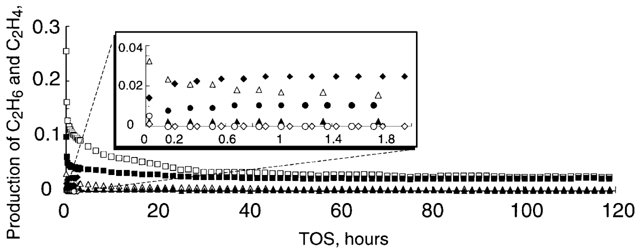

FIG. 12. Ethene and ethane formation during propane dehydrogenation: (□) ethane formation, Pt/Al_2O_3; (■) ethene formation, Pt/Al_2O_3; (+) ethane formation, $Pt{-}Sn/Al_2O_3$; (▲) ethene formation, $Pt{-}Sn/Al_2O_3$; (◯) ethane formation, Sn/Al_2O_3; (●) ethene formation, Sn/Al_2O_3; (◇) ethane formation, Al_2O_3; (◆) ethene formation, Al_2O_3. The reaction mixture contained 20 ml/min C_3H_8, 6 ml/min H_2, and 40 ml/min N_2. The temperature was 789 K and 10 mg of catalyst was used in each run.

the metal was added to the alumina. Tin in known to reduce the acidity of the carrier (2, 3, 30, 31) and to decrease hydrogenolysis reactions on the metal (3, 32).

We suggest the following explanation for the ethane and ethene formation results. Ethene is mainly formed from cracking on the carrier. The slow deactivation is caused by coke accumulated on the active sites. On the Pt catalyst a part of the ethene is formed on the metal, but this process deactivates quickly. The ethane is formed by hydrogenolysis of propane and by hydrogenation of ethene, with both reactions taking place on the metal. Ethane is not formed on the carrier except very early in the experiments. The observation that the ethane formation deactivates faster than the propane dehydrogenation can be explained if we consider that the former process is taking place on larger ensembles than the latter (33–35) and that coke also is formed preferentially on these sites (34, 36, 37).

The Effect of Hydrogen

Hydrogen has proven to be very efficient in maintaining the activity of the catalyst and also suppressing the coke formation. On the other hand, it was not possible to remove any coke after the reaction stopped. The conclusion must be that hydrogen is active in preventing coke formation but does not remove any significant amount of coke already formed. The latter does not agree with the results of Biswas *et al.* (38). By treatment with hydrogen at 773 K they succeeded in removing a considerable part of the coke formed on a Pt/Al_2O_3 catalyst by cyclohexane conversion at 753 K. The coke formed in the experiments presented in this study has, because of a higher temperature and longer time on stream during the coking, probably been more deeply dehydrogenated and strongly bound to the catalyst. During the reaction, on the other hand, the formation of coke precursors is suppressed by hydrogen, and what Biswas *et al.* called reversible coke, can be removed by hydrogenation (38). This explains why hydrogen helps maintain the catalytic activity.

CONCLUSIONS

Three different peaks were detected in the TPO profiles. The first was found to be coke on and in the vicinity of the metal. The second peak was coke on the carrier, and the third one was graphitic coke on the carrier. We suggested a model which proposes that the coke observed is not responsible for the deactivation but formed in parallel. The relation between the deactivating coke (Coke B) and the major part of the coke (Coke A) is independent of gas composition, but it is dependent on the temperature. The graphitic type of coke on the carrier is formed via a separate mechanism, independent of the deactivation of the main reaction. Hydrogen can reduce the deactivation rate and formation of the main part of the coke by suppressing coke precursor formation, but it cannot remove the coke already formed on the catalyst.

ACKNOWLEDGMENT

This work was supported by the Nordic Council, in the Petroleum program.

REFERENCES

1. Loc, L. C., Gaidai, N. A., and Kiperman, S. L., “Proceedings, 9th Int. Congr. Catal.” (M. J. Phillips and M. Ternan, Eds.), Vol. 3, p. 1261. Chem. Inst. Canada, Ottawa, Ont., 1988.
2. Burch, R., and Garla, L. C., *J. Catal.* **71**, 360 (1981).
3. Wilde, M., Anders, K., and Neubauer, H.-D., *Erdöl Erdgas Kohle* **110**, 463 (1994).
4. Beltramini, J., and Trimm, D. L., *Appl. Catal.* **31**, 113 (1987).
5. Praserthdam, P., Panchareon, U., and Tscheikuna, J., *Kenkyu Hokoku—Asahi Garasu Zaidan* **61**, 313 (1992).
6. Sanfilippo, D., Fusco, G., and Buonomo, F., “Proceedings, Int. Conf. Pet. Refin. Petrochem. Process.,” p. 689 (X. Hou, Ed.). Int. Acad. Publ., Beijing, 1991.
7. Mieville, R. L., *Stud. Surf. Sci. Catal.* **68**, 151 (1991).
8. Lin, L., Zhang, T., Zang, J., and Xu, Z., *Appl. Catal.* **67**, 11 (1990).
9. Zhang, T., Zang, J., and Lin, L., *Stud. Surf. Sci. Catal.* **68**, 143 (1991).
10. Sárkány, A., Lieske, H., Szilágyi, T., and Tóth, L., “Proceedings, 8th Int. Congr. Catal., 1984,” Vol. 2, p. II613. Verlag Chemie, Weinheim, Germany, 1984.
11. Afonso, J. C., Schmal, M., and Fréty, R., *Fuel Process. Technol.* **41**, 13 (1994).
12. Beltramini, J. N., and Datta, R., *React. Kinet. Catal. Lett.* **44**, 353 (1991).
13. Bariås, O. A., Holmen, A., and Blekkan, E. A., *Stud. Surf. Sci. Catal.* **88**, 519 (1994).
14. Völter, J., Lietz, G., Uhlemann, M., and Hermann, M., *J. Catal.* **68**, 42 (1981).
15. Datka, J., and Eischens, R. P., *Stud. Surf. Sci. Catal.* **68**, 127 (1991).
16. Lok, L. K., Kiperman, S. L., Kogan, S. B., Podkletnova, N. M., and Gaidai, N. A., *Kinetics Catal.* **29**(5), 989 (1988).
17. Larsson, M., Andersson, B., Bariås, O. A., and Holmen, A., *Stud. Surf. Sci. Catal.* **88**, 233 (1994).
18. Holmen, A., Lindvaag, O. A., and Trimm, D. L., ACS Symp. Ser., Vol. 202, p. 45, *Am. Chem. Soc.,* Washington, DC, 1982.
19. Montgomery, D. C., “Design and Analysis of Experiments,” 2nd ed., Wiley, New York, 1984.
20. Wrammerfors, Å., and Andersson, B., *J. Catal.* **147**, 82 (1994).
21. Wrammerfors, Å., and Andersson, B., *J. Catal.* **146**, 34 (1994).
22. Duprez, D., Hadj-Aissa, M., and Barbier, J., *Appl. Catal.* **49**, 67 (1989).
23. Duprez, D., Hadj-Aissa, M., and Barbier, J., *Appl. Catal.* **49**, 75 (1989).
24. Liu, Y., Yang, J., and Yang, G., “Proceedings, Int. Conf. Pet. Refin. Petrochem. Process.,” p. 362 (X. Hou, Ed.). Int. Acad. Publ., Beijing, 1991.
25. Basso, T. C., Zhang, Z., and Sachtler, W. M. H., *Appl. Catal.* **79**, 227 (1991).
26. Barbier, J., *Stud. Surf. Sci. Catal.* **34**, 1 (1987).
27. Lieske, H., Sarkany, A., and Voelter, J., *Appl. Catal.* **30**, 69 (1987).
28. Querini, C. A., and Fung, S. C., *Appl. Catal. A* **117**, 53 (1994).
29. Bacaud, R., Charcosset, H., Guenin, M., Torréllas-Hidalgo, R., and Tournayan, L., *Appl. Catal.* **1**, 81 (1981).

30. Shen, J., Cortright, R. D., Chen, Y., and Dumesic, J. A., *Catal. Lett.* **26**, 247 (1994).
31. Srinivasan, R., and Davis, B. H., *J. Mol. Catal.* **88**, 343 (1994).
32. Coq, B., and Figueras, F., *J. Catal.* **85**, 197 (1984).
33. Biloen, P., Dautzenberg, F. M., and Sachtler, W. M. H., *J. Catal.* **50**, 77 (1977).
34. Ribeiro, F. H., Bonivardi, A. L., Kim, C., and Somorjai, G. A., *J. Catal.* **150**, 186 (1994).
35. Biswas, J., Bickle, G. M., Gray, P. G., Do, D. D., and Barbier, J., *Catal. Rev.—Sci. Eng.* **30**, 161 (1988).
36. Barbier, J., Corro, G., Zhang, Y., Bournonville, J. P., and Franck, J. P., *Appl. Catal.* **13**, 245 (1985).
37. Ribeiro, F. H., Bonivardi, A. L., and Somorjai, G. A., *Catal. Lett.* **27**, 1 (1994).
38. Biswas, J., Gray, P. G., and Do, D. D., *Appl. Catal.* **32**, 249 (1987).